Kuwait J.Sci., Vol.50, No.(1A),January.2023,pp(1-12)

Mass attenuation coefficient, stopping power, and penetrating distance calculations via Monte Carlo simulations for cell membranes

Yiğit Ali Üncü[1], Gençay Sevim[2], Osman Ağar[3], Hasan Özdoğan[4,*]

[1]*Dept. of Biomedical Equipment Technology, Akdeniz University, Vocational School of Technical Sciences, 07070, Antalya, Turkey*

[2]*Dept. of Medical Imaging Techniques, Ufuk University, Vocational School of Health Services, 06805, Ankara, Turkey*

[3]*Dept. of Medical Imaging Techniques, Karamanoğlu Mehmetbey University, Vocational School of Health Services, 70100, Karaman, Turkey*

[4]*Dept. of Medical Imaging Techniques, Antalya Bilim University, Vocational School of Health Services, 07190, Antalya, Turkey*

[*]*Corresponding author: hasan.ozdogan@antalya.edu.tr*

Abstract

The Monte Carlo (MC) method is a computer simulation that is widely used in different disciplines including physics, biology, biophysics, medical imaging, biomedical engineering, etc. In addition, MC method is often used to simulate the interaction of radiation with cells, tissues, and the environment. In the present study, mass attenuation coefficient, stopping power, and penetrating distance calculations were performed for cell membranes having an approximately 60-100Å thickness. These calculations have been done for lipid bilayer structure of cell membrane via MC techniques employing two of the most known computer-aided calculation and simulation software which are MC methods such as SRIM-2013 (The Stopping and Range of Ions in Matter) and MCNPv6 (Monte Carlo N-Particle) with XCOM software. Stopping power and penetrating distance calculations were obtained using SRIM-2013. Also, both XCOM software and MCNPv6 simulation code were used to obtain photon interaction parameters within the energy range of 0.01 – 10000keV. Obtained all results from different codes have been visualized by graphing for evaluation.

Keywords: Cell membrane; mass attenuation coefficient; penetrating distance; stopping power; simulation software

1. Introduction

The cell has a plasma membrane on the surface of its cytoplasm. The cell membrane (plasma membrane) is a structure that surrounds the cell and is located between the cytosol and the extracellular environment (Korn, 1968; Stryer, 1995). The main function of cell membrane is to

set the boundaries of cell and to separate the parts of cell. While separating the inner and outer environments of the cells, membranes also control the entry and exit of certain substances for the cell. Various nutrients, gases, water, and other substances enter and exit the cell. Since membranes have different permeability to different substances, each substance enters and leaves the cell in different ways. The cells generally receive electrical and chemical signals from the environment. The cell membrane is responsible for receiving signals and responding to them. The molecules or structures required for these functions are located in the structures of membrane (Brady *et al.,* 2005; Félix, 2014; Grecco *et al*., 2011; Korn, 1968).

Using an electron microscope, it was seen that they consist of 3 layers in their chemical structure. The upper and lower layers consist of hydrophilic groups, whereas the middle layer consists of hydrophobic groups. This structure is also the same in the plasma membrane that limits the cell and in other organelle membranes. For this reason, the term "unit membrane" is used as a general term (Félix, 2014; Korn, 1968; Stryer, 1995).

The cell membrane consists of molecules having lipid content such as phospholipids, glycolipids, cholesterol, proteins (Membrane proteins), and carbohydrates (Glycocalyx). Phospholipids made of glycerol are called phosphoglycerides. A phosphoglyceride contains glycerol, two fatty acid chains, and phosphorylated alcohol (Félix, 2014).

Membrane proteins forming the basic structure of biological membranes such as lipid bi-membranes fulfill the most specific functions in membranes. Therefore, proteins are molecules that give the membrane its characteristic structure. Membrane properties vary depending on the amount and type of proteins. Most plasma membranes are 50% lipid and 50% protein by weight, with the carbohydrate portions of glycolipids and glycoproteins constituting 5 to 10% of the membrane mass. Since proteins are much larger than lipids, this ratio is equivalent to approximately one protein molecule for every 50 to 100 lipid molecules (Lodish *et al.,* 2000). In addition, proteins participating in the structure of the cell membrane play a role as integral proteins embedded in phospholipid layers or as peripheral proteins attached to the inner or outer surface of these layers (Brady *et al.,* 2005; Hung & Link, 2011; Korn, 1968).

In the present study, the mass attenuation coefficients and stopping power of cell membrane were calculated by using Monte Carlo Simulation methods. In the calculations, SRIM-2013 (The Stopping and Range of Ions in Matter) (Ziegler *et al,.* 2010) and MCNPv6 (Monte Carlo N-Particle) (Goorley *et al.,* 2013) codes were used. The calculation results have been compared and the results have been graphed for better visual understanding.

2. Material and Methods

In the present study, stopping power, penetrating distance, and mass attenuation coefficients were calculated for cell membranes by using MC simulation methods. SRIM-2013 was used for the stopping power and penetrating distance, whereas MCNPv6 and XCOM were used for the mass attenuation coefficient. MC method is a useful analysis tool and is widely used in different disciplines including physics, biology, biophysics, medical imaging, biomedical engineering, etc. The application of MC method to a problem is based on the idea that the problem is simulated by

using random numbers and the parameter to be calculated is approximated by making use of the results obtained from these simulations.

It is well-known that cell membranes consist of 50% lipid and 50% protein by weight and these rates vary at different points of the plasma membrane (density = 1.12 g/cm^3) (Lodish *et al.,* 2000). The elemental components of the cell membrane, which are quite complex and different in every cell, make exact modeling difficult. Considering this difficulty and the 50% lipid concentration of the membrane, the elemental component of the phospholipid bilayer was used in modeling the phospholipid bilayer structure of the cell membrane (Table 1). For this purpose, the average element amount of modeled phospholipid was calculated by using different phospholipid derivatives (Mashaghi *et al.,* 2012; Ulmschneider *et al*., 2005; Yang, 2014). This average amount of elements was determined separately for both the hydrophilic head and hydrophobic tail of the phospholipid. The average chemical structure was used in determining the amount of elements in each structure (Ulmschneider *et al.i* 2005).

Table 1. Average elemental component of modelled phospholipid bilayer cell membrane

Lipid Structure	Element	Number of Element per unit
Hydrophilic Head (0.7 – 1 nm)	Hydrogen	18
	Oxygen	8
	Carbon	10
	Nitrogen	1
	Phosphor	1
Hydrophobic Tail (1.5 – 2 nm)	Hydrogen	66
	Carbon	36
	Oxygen	2
Sum of Phospholipid Bilayer	Hydrogen	168
	Oxygen	20
	Carbon	92
	Nitrogen	2
	Phosphor	2

SRIM-2013 code was used in order to calculate the penetrating distance and stopping power using the Equations (1-10). Lambert-Beer law equation is presented in Equation (1),

$$I = I_0 e^{-\mu x} \quad (1)$$

μ (cm^{-1}) is the linear attenuation coefficient for a material, where I is the attenuated photon intensity, I_o is non-attenuated photon intensity, and x (cm) is the thickness. The following equation for the linear attenuation coefficient is obtained by mathematically rearranging the Equation (2);

$$\mu = \frac{1}{x} \ln(I_0/I) \quad (2)$$

Using the density of target materials (ρ), the mass attenuation coefficients are calculated using Equation (3).

$$\mu/\rho = \frac{1}{\rho x} \ln(I_0/I) \quad (3)$$

As charged particles move through the material, they perform many interactions before consuming all their kinetic energy. During these interactions, the charged particle' trajectory of motion may vary such as elastic and inelastic collisions. It can lose some of its energy by transferring it to the collision loss or radiative loss as photons. The loss of energy of a charged particle trying to move through a material depends on the characteristic properties of the material as the particle.

The linear stopping power (*-dE/dx*) is the rate of energy loss per unit length of motion of a charged particle through matter. Stopping power is a characteristic feature peculiar to the material. Average energy loss per unit motion length of charged particles is $dE/d\ell$. For a certain energy loss, the cross-section expression σ_{ni} and the energy loss ΔE_{ni} are expressed as shown in Equation (4) and the sum of all possible *i* states (Podgorsak, 2016).

$$-\frac{\mathrm{d}E}{\mathrm{d}\ell} = \sum_i N_i \sum_n \Delta E_{ni} \sigma_{ni} \quad (4)$$

Where, N_i refers to the atomic density and can be valued in two different ways due to the possible sizes of i. First, it is the number of atoms per unit volume that allows the $-dE/d\ell$ expression to be defined as the energy loss per unit movement length in the material, in other words, linear stopping power *-dE/dx*. The typical unit of linear stopping power expression is MeV/cm, although *keV/μm* is also used in some cases. Then, it is the number of atoms per unit mass that allows the expression dE/dl to be defined as the energy loss per unit g/cm^2 in the material, the mass stopping power $S = -(1/\rho)\mathrm{dE/dx}$. The typical unit of mass stopping power expression is *MeV.cm2/g* (Podgorsak, 2016).

Regarding the charged particle interaction, there are two types of stopping forces known as radiative (nuclear) stopping power and collision (electronic or ionized) stopping power. Radiation stopping power is the stopping power arising from the Coulomb interactions between atomic nuclei of matter and charged particles. In addition, the charged particles such as electrons and positrons experience significant energy loss through these interactions, commonly referred as Bremsstrahlung interactions. For heavily charged particles such as protons and alpha, the radiative stopping power loss is negligible when compared to the collision stopping power. The power to stop the collision is the stopping power created by the Coulomb interactions between the orbital electrons of matter and the charged particle. Both lightly and heavily charged particles experience

this interaction that causes ionization or excitation in matter atoms as a result of the energy transfer between charged particles and orbital electrons.

The total stopping power for a charged particle having kinetic energy E_K moving through a material with the atomic number Z, which is S_{total}, is generally the sum of radiative stopping power $S_{radiative}$ and collision stopping power $S_{collision}$, as expressed in Equation (5).

$$S_{total} = S_{radiative} + S_{collision} \tag{5}$$

The collision stopping power can be expressed as in Equation (6), divided into two subcomponents as $S_{collision}^{soft}$ and $\mathrm{S}_{\mathrm{collision}}^{\mathrm{hard}}$.

$$S_{collision} = S_{collision}^{soft} + S_{collision}^{hard} \tag{6}$$

By combining Equations (5-6), the total stopping power can be expressed as in Equation (7).

$$S_{total} = S_{radiative} + S_{collision} = S_{radiative} + S_{collision}^{soft} + S_{collision}^{hard} \tag{7}$$

Energy transfer from energetic heavily charged particles to matter occurs mainly through Coulomb interactions (collision or electronic loss) between the nucleus and orbital electrons of charged particles. Inelastic Coulomb interactions (radiation loss) between heavily charged particles and nuclei of matter atoms are negligible and, therefore, they are ignored (Podgorsak, 2016).

The total collision stopping power is expressed as the sum of soft and hard collisions in Equation (8),

$$\begin{aligned} S_{collision} &= S_{collision}^{soft} + S_{collision}^{hard} \\ &= 2\pi \frac{ZN_A}{A}\left(\frac{e^2}{4\pi\varepsilon_0}\right)^2 \frac{z^2}{m_e c^2 \beta^2} \times \left\{ ln\frac{2m_e c^2 \beta^2 \eta}{(1-\beta^2)I^2} + ln\frac{2m_e c^2 \beta^2}{(1-\beta^2)\eta} - 2\beta^2 \right\} \\ &= 4\pi \frac{ZN_A}{A}\left(\frac{c^2}{4\pi\varepsilon_0}\right)^2 \frac{z^2}{m_e e^2 \beta^2} \left\{ ln\frac{2m_e c^2}{I} + ln\frac{\beta^2}{1-\beta^2} - \beta^2 \right\} \\ &= C_0 \frac{z^2}{A\beta^2} Z \left\{ ln\frac{2m_e c^2}{I} + ln\frac{\beta^2}{1-\beta^2} - \beta^2 \right\} \end{aligned} \tag{8}$$

where, η refers to the energy separating the soft and hard collisions that would disappear in the final state of the equation; C_0, r_e refers to the collision stopping power constant shown by Equation (9), where r_e is the classical electron radius $(r_e = e^2/(4\pi\varepsilon_0 m_e c^2) = 2.818\, fm)$ (Podgorsak, 2016).

$$C_0 = 4\pi N_A \left(\frac{e^2}{4\pi\varepsilon_0}\right)^2 \frac{1}{m_e c^2} = 4\pi N_A r_e^2 m_e c^2 = 0{,}3071 \text{ MeV.cm}^2/\text{mol} \quad (9)$$

The average atomic stopping power of a mixture will be expressed by Equation (10) (Evans, 1955).

$$(\mathrm{S_n})_{\mathrm{av}} = \frac{(ds)_0}{(ds)_{\mathrm{av}}}\frac{N_0}{N} = \frac{B_{\mathrm{av}}}{B_0} = n_1\mathrm{S}_1 + n_2\mathrm{S}_2 + n_3\mathrm{S}_3 + \cdots \quad (10)$$

where, N refers to the number of atoms in one cm^3 of the mixture or compound selected as the stopping; values of n_1, n_2, n_3,… ; S_1, S_2, S_3,… express the atomic ratios of atoms having stopping power values in the material.

SRIM-2013 provides many calculations including range, collision, penetration, stopping powers, and straggling distributions for any ion. In the present study, using Ion Stopping and Range Tables application in the SRIM-2013 package for each ion, stopping powers of a cell membrane and ions' penetration distances were theoretically calculated. Lipid membrane structure was modelled as an elemental target and 5 different ions were used at 0.01 – 10000 keV. The reason for modelling such a wide range of energy is to be able to derive a wide scale of the stopping power for the cell membrane and to be able to determine the minimum energies of ions that can penetrate the phospholipid membrane.

MCNPv6, which uses the Monte Carlo technique, is a program that can simulate cases such as particle-matter interaction and nuclear reactions, in which it is not possible to get exact and accurate results by using analytical algorithms. It is a general Monte Carlo transport code that solves the time-dependent continuous energy transfer of radiation such as neutron, photon, electrons in three-dimensional geometry. In MCNPv6, the input file contains the information of geometry description, description of materials and selection of cross-section evaluations, location, and properties of a radiation source, type of desired response or tasks, and variance reduction techniques.

The geometry used in MCNPv6 calculations is presented in Figure 1. In this study, the simulations include a point photon source placed in a cylinder (r=0.5 cm; h=1cm) which emits mono-energetic photons directed in a parallel manner toward a cylindrical sample 100 cm away from isotropic point source to calculate the counts of photons entering the detector per $MeVcm^2s^{-1}$. All the components of the problem geometry were surrounded by a vacuum sphere to avoid interactions in materials other than the sample. The "F4" tally gives the average photon flux in the detection field. In, the number of histories (NPS variable) used in the MCNPv6 simulations is 5.10^6. The test of the recent MCNPX simulation has been implemented by using the D00205ALLCP03 MCNPXDATA package is included of DLC-200/MCNPDATA cross-section lib.s. Also, Population Control Methods have been employed as variance reduction in MCNP simulations. These methods artificially increase/decrease the number of particles in spatial or energy regions that are important/unimportant to the tally score. The weight cutoff has been used

for variance reduction. In this study, photons with energies below 1 keV are neglected. All the calculations were performed using computer hardware (Intel Core I7 CPU 2.6 GHz). First, calculations were performed in the absence of a cell membrane, which gives us I_0. Then, the cell membrane was placed between the source and the detector and the flux through the membrane was calculated (I). After the calculations, the Beer-Lambert formula was used in order to obtain the mass attenuation coefficients.

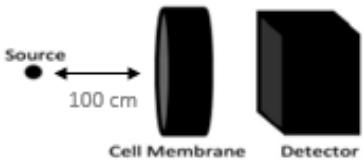

Fig. 1. The geometry which is used in MCNPv6 simulations

3. Results

Using Monte Carlo Simulation methods, the stopping power, penetrating distance, and mass attenuation coefficients of cell membrane were calculated in this paper. Stopping power and penetrating distance calculations, which were obtained using SRIM-2013, are illustrated in Figures 2 and 3. Moreover, the minimum projectile energy required to pass through the membrane is presented in Tables 2 and 3. Mass attenuation coefficients of the cell membrane are shown in Figure 4. Stopping power calculations versus projectile energy is shown in Figure 2. Alpha and helium-3 have the highest stopping power results, followed by tritium, deuterium, and proton, respectively. The charge of the projectile particle is directly proportional to the stopping power.

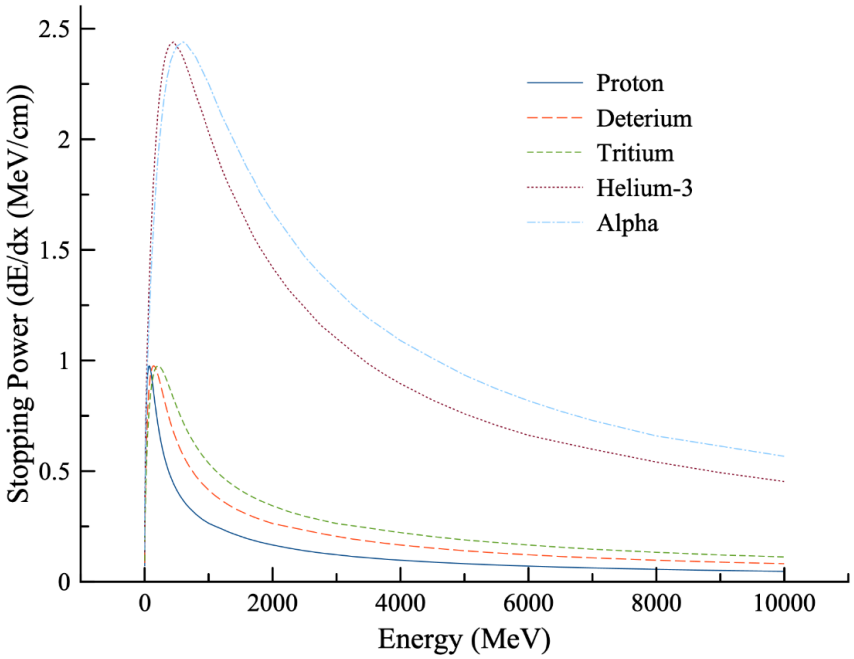

Fig. 2. Stopping power calculations of cell membrane

Penetrating distance calculations of charged particles within the cell membrane are illustrated in Figure 3. As expected, alpha has the smallest range, which is in parallel with tritium, deuterium, and proton stopping power results. On the contrary with the stopping power results, penetrating distance decreased as the charge of projectiles increased. It is well known that the cell membrane thickness is approximately 60-100 Å (Greenberg *et al.,* 2002). The minimum energy levels for the charged particles to pass through the membrane are given in Tables 2 and 3.

Table 2. Minimum energy range that can pass through the membrane for proton, deuterium, and tritium

Ion Energy (eV)	Proton Projected Range (Å)	Deuterium Projected Range(Å)	Tritium Projected Range(Å)
140	58	58	58
150	61	62	62
160	65	66	66
170	68	69	69
180	72	73	73
200	79	80	80
225	88	89	89
250	97	99	98
275	106	108	107

Table 3. Minimum energy range that can pass through the membrane for helium-3 and alpha

Ion Energy (eV)	Projected Range 3He (Å)	Projected Range ∝ (Å)
275	61	61
300	65	66
325	70	70
350	75	75
375	79	79
400	84	84
450	93	93
500	103	102

According to these calculations, the ion energy interval of 140-275 eV is enough for proton, deuterium, and tritium to pass through the cell membrane, whereas a higher ion energy interval (275-500 eV) is required for helium-3 and alpha to pass through the membrane.

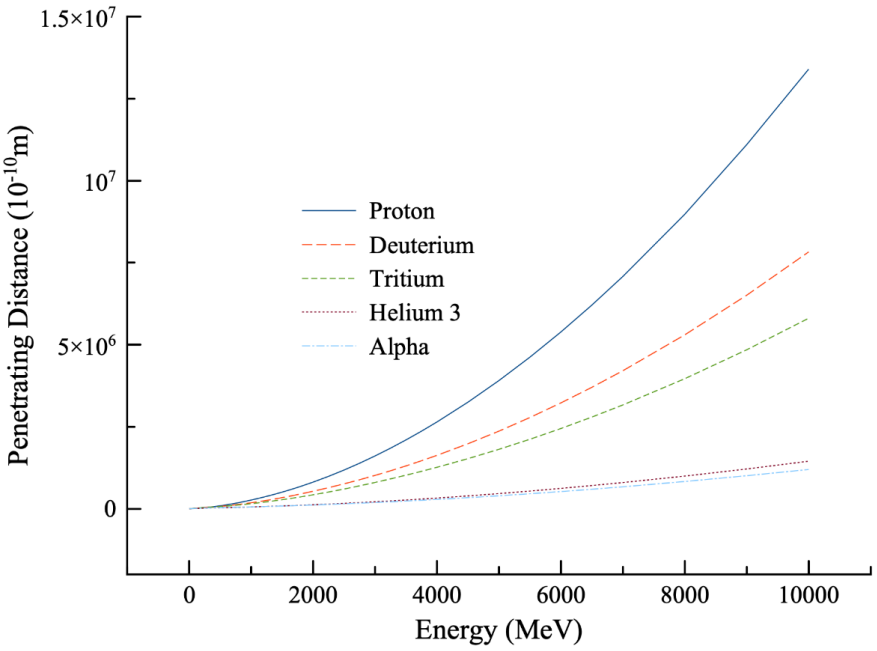

Fig. 3. Penetrating distance calculations of charged particles within the cell membrane

The mass attenuation coefficients of the cell at 0.05, 0.1, 0.2, 0.3, 0.4, 0.5, 0.6, 0.7, 0.8, 0.9, 1.0, 2.0, 4.0, 6.0, 8.0, and 10.0 MeV photon energies were calculated by using MCNPv6 and XCOM programs and the following graphs were obtained (Table 4). The comparison of MCNPv6 and XCOM results show the mass attenuation coefficients of the cell membrane in Figure 4. In addition, relative deviations (RD) of MCNP6 and WinXCOM μ/ρ values were calculated by using following equation;

$$RD = |\,(\mu/\rho WinXCom - \mu/\rho MCNP6)/\mu/\rho WinXCom * 100| \qquad (11)$$

As seen in Table 2, the RDs of the results of two methods at all energies is generally < 2%. Therefore, it is clear that XCOM, which is web-based computational tool (Berger *et al.,* 2010), results and MCNPv6 results are in harmony with each other. Additionally, mass attenuation coefficients of the cell membrane sharply decrease throughout the low energy region for less than 400 keV while tending to be almost constant for the photon energy region of 400 <E < 3000 keV. The basic reason of this trend can be attributed to principal radiation physics concepts. One of three, the photoelectric absorption is the most dominant interaction mechanism over 50 keV < E < 400 keV as compared to Compton scattering mechanism, where is more effective for E > 400 keV. Both processes are related to the energy as E−3.5 and E−1, respectively. Also, the above-mentioned rapid and linear declines are resulting from the dependence of these processes with the atomic number as Z4−5 and Z, respectively. These mass attenuation coefficients are close to zero in the high energy region where pair production which has cross-section depending on Z2 are dominant.

Table 4. Mass attenuation coefficient results of cell membrane

Energy (MeV)	μ/ρ (cm²/g)		RD
	MCNP6	XCOM	
0.05	0.2175	0.2183	0.36
0.1	0.1692	0.1678	0.82
0.2	0.1363	0.1352	0.78
0.3	0.1172	0.1172	0.04
0.4	0.1050	0.1049	0.05
0.5	0.0965	0.0957	0.77
0.6	0.0890	0.0885	0.60
0.7	0.0832	0.0827	0.67
0.8	0.0784	0.0777	0.92
0.9	0.0737	0.0735	0.22
1.0	0.0705	0.0699	0.86
2.0	0.0493	0.0488	1.01
4.0	0.0328	0.0334	1.66
6.0	0.0270	0.0270	0.06
8.0	0.0233	0.0235	0.86
10.0	0.0212	0.0213	0.66

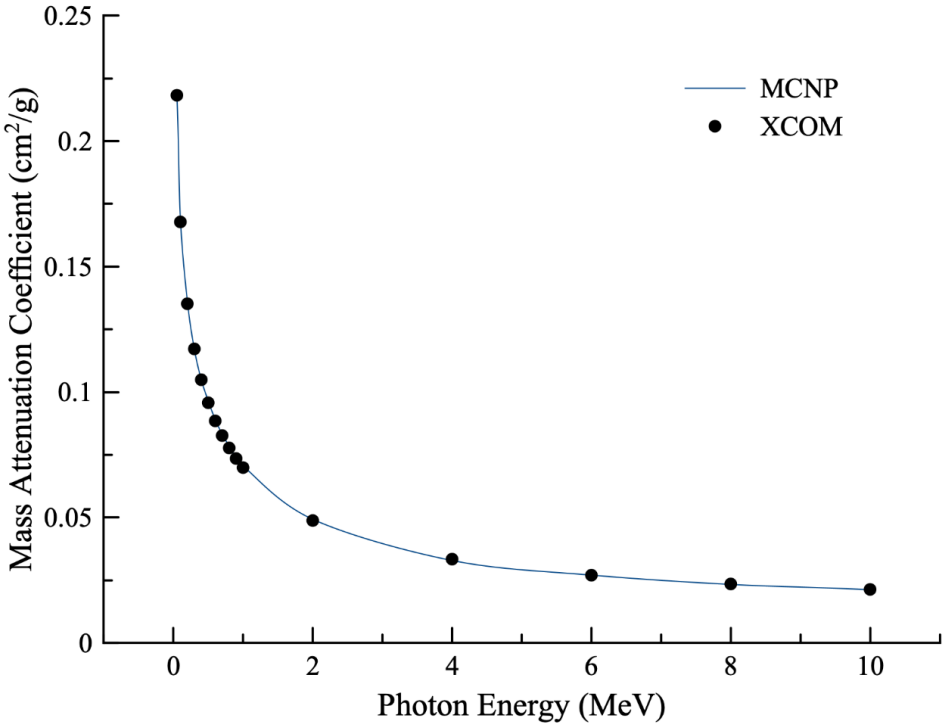

Fig. 4. Mass attenuation coefficient calculations for cell membrane

4. Conclusions

In this study, we focused on how the radiation affects the cell membrane. The radiation can damage the cell membrane and the effect of radiation on the cells will be investigated as a major topic in future clinical studies. Stopping power is the retarding force acting on charged particles (typically helium-3, tritium, deuterium, and proton particles) causing loss of particle energy due to interaction with cell membrane. It is known that the cell membrane thickness is approximately 60-100 Å. The range of a particle moving through the cell thickness depends on the excess energy of the particle. The stopping power increases with the excess energy of the particle in Figure 2.

The present study revealed the minimum energy range that can pass through the membrane for proton, deuterium, and tritium for 58-108 Å cell thickness (Table 2) and can pass through the membrane for helium-3 and alpha for 61-103 Å (Table 3). As seen in Figure 3, the penetrating distance of charged particles impinging in the cell membrane was calculated using SRIM-2013. This fit is important for the validation of the MCNPv6 and the result is corroborated by the result that the Monte Carlo method is a powerful tool in such studies. There is no experimental or theoretical study on the mass attenuation coefficient and stopping powers of the cell membrane in the literature. It is thought that the findings achieved in the present study can be used with researchers studying in radiobiology.

References

Brady, S., Siegel, G., Albers, R. W. & Price, D. L. (2005) Basic neurochemistry: molecular, cellular and medical aspects. Elsevier. Pp. 26.

Berger, M.J., Hubbell, J.H., Seltzer, S.M., Chang, J., Coursey, J.S., Sukumar, R., Zucker, D.S. & Olsen, K. (2010) XCOM: Photon Cross Section Database, National Institute of Standards and Technology, Gaithersburg, MD.

Evans, R.D. (1955) The Atomic Nucleus. McGraw Hill, New York. Pp. 972.

Félix, M.D. (2014) The basic structure and dynamics of cell membranes: An update of the Singer–Nicolson model. Biochimica et Biophysica Acta (BBA) – Biomembranes, 1838(6):1467-1476.

Goorley, J.T., James, M.R., Booth, T.E., Brown, F.B., Bull, J.S., Cox, L.J., Durkee, Jr., Joe W., Elson, J.S., Fensin, M.L., Forster, III, Robert A., Hendricks, J.S., Hughes, III.H. G., Johns, R.C., Kiedrowski, B.C., Martz, R.L., Mashnik, S.G., McKinney, G.W., Pelowitz, D.B., Prael, R.E., Sweezy, J. Ed., Waters, L.S., Wilcox, T., & Zukaitis, A.J. (2013) Initial MCNP6 Release Overview - MCNP6 version 1.0. United States.

Grecco, H.E., Schmick, M. & Bastiaens, P.I. (2011) Signaling from the living plasma membrane. Cell, 144: 897–909.

Greenberg, A., Breneman, C. M. & Liebman, J. F. (2002) The amide linkage: Structural significance in chemistry, biochemistry, and materials science. Wiley, New York. Pp. 599.

Hung, M.C. & Link, W. (2011) Protein localization in disease and therapy. Journal of Cell Science, 124(Pt 20):3381–3392.

Korn, E.D. (1968) Structure and Function of the Plasma Membrane: A biochemical perspective. Journal of General Physiology, 52(1):257-278.

Lodish, H., Berk, A., Zipursky, S.L., Matsudaira, P., Baltimore, D. & Darnell, J. (2000) Photosynthetic Stages and Light-Absorbing Pigments. Molecular Cell Biology. W. H. Freeman and Company, New York. Pp. 152.

Mashaghi, A., Partovi-Azar, P., Jadidi, T., Nafari, N., Maass, P., Tabar, M.R.R., Bonn, M. & Bakker, H.J. (2012) Hydration strongly affects the molecular and electronic structure of membrane phospholipids. The Journal of chemical physics, 136(11): 114709-5.

Podgorsak, E.B. (2016) Radiation Physics for Medical Physicists. Springer, Switzerland. Pp. 906.

Sharma, A., Sayyed, M.I., Ağar, O. & Tekin, H.O. (2019) Simulation of shielding parameters for TeO2 WO3 GeO2 glasses using FLUKA code. Results in Physics, 13:102199.

Stryer, L. (1995) Biochemistry.W. H. Freeman and Company, New York. Pp. 263.

Ulmschneider, M. B., Sansom, M. S., & Di Nola, A. (2005) Properties of integral membrane protein structures: derivation of an implicit membrane potential. Proteins: Structure, Function, and Bioinformatics, 59(2): 252-265.

Yang, Y., & Hu, B. (2014) Bio-based chemicals from biorefining : Lipid and wax conversion and utilization. Advances in Biorefineries: Biomass and Waste Supply Chain Exploitation, Pp. 693-720. Elsevier Ltd.

Ziegler, J.F., Ziegler, M.D. & Biersack, J.P. (2010) SRIM - The Stopping and Range of Ions in Matter. Nuclear Instruments and Methods in Physics Research, Section B: Beam Interactions with Materials and Atoms, 268(11–12):1818–23.

Submitted: 18/09/2021
Revised: 19/12/2021
Accepted: 2612/2021
DOI: 10.48129/kjs.15657